

# CAMA: Enhancing Multimodal In-Context Learning with Context-Aware Modulated Attention

Yanshu Li<sup>1</sup>, Jianjiang Yang<sup>2</sup>, Bozheng Li<sup>1</sup>, Ruixiang Tang<sup>3</sup>

<sup>1</sup>Brown University, <sup>2</sup>University of Bristol, <sup>3</sup>Rutgers University  
yanshu\_li1@brown.edu

## Abstract

Multimodal in-context learning (ICL) enables large vision–language models (LVLMs) to efficiently adapt to novel tasks, supporting a wide array of real-world applications. However, multimodal ICL remains unstable, and current research largely focuses on optimizing sequence configuration while overlooking the internal mechanisms of LVLMs. In this work, we first provide a theoretical analysis of attentional dynamics in multimodal ICL and identify three core limitations of standard attention that ICL impair performance. To address these challenges, we propose Context-Aware Modulated Attention (CAMA), a simple yet effective plug-and-play method for directly calibrating LVLM attention logits. CAMA is training-free and can be seamlessly applied to various open-source LVLMs. We evaluate CAMA on four LVLMs across six benchmarks, demonstrating its effectiveness and generality. CAMA opens new opportunities for deeper exploration and targeted utilization of LVLM attention dynamics to advance multimodal reasoning.

## 1 Introduction

Motivated by LLMs’ success, researchers fuse vision encoders with lightweight modules (e.g., MLPs) to integrate visual features into the LLM’s hidden space, forming Large Vision–Language Models (LVLMs) (Ye et al., 2023; Liu et al., 2023a; Bai et al., 2023). Recent advances in architecture and training have enabled LVLMs to process multiple images and perform interleaved cross-modal reasoning (Laurençon et al., 2024a; Bai et al., 2025; Chen et al., 2025). Consequently, multimodal in-context learning (ICL) has emerged as a crucial application (Doveh et al., 2024a,b). By incorporating few examples directly into the input prompt, LVLMs can rapidly adapt to novel tasks without any parameter updates. This highly efficient and effective learning paradigm substantially enhances the practical utility of LVLMs.

While ICL can enhance certain vision–language tasks, its performance is notoriously unstable and can even fall below zero-shot baselines. This volatility intensifies as the number of in-context demonstrations (ICDs) grows or when tackling complex cross-modal reasoning. Numerous studies show that LVLM performance is critically dependent on the configuration of the sequence in context: subtle factors such as ICD order and structure can dramatically influence results (Liu et al., 2021; Gao et al., 2021; Lu et al., 2022). In response, many methods focus on optimizing sequence configuration to identify an ‘ideal’ ordering for effective ICL (Li et al., 2023a; Yang et al., 2024). However, due to their neglect of LVLMs’ internal mechanisms, these methods often cannot fundamentally resolve the inherent instability of ICL. Some recent efforts have begun to tackle the issue through attention-based modifications, but the complexity of multimodal ICL still poses significant challenges to these solutions (Liu et al., 2024; Tian et al., 2025).

To bridge this gap, we first present a theoretical analysis of attentional dynamics, pinpointing three core limitations of standard attention in multimodal ICL: (1) inadequate intra-ICD cross-modal alignment, (2) imprecise query-sample-guided attention, and (3) neglected inter-ICD influences. To effectively mitigate these three limitations, we introduce Context-Aware Modulated Attention (CAMA), a training-free, inference-time attention-calibration method. CAMA directly adjusts the raw attention logits computed by the LVLM by integrating a Query-ICD Joint Affinity Score, which holistically assesses relevance and implicitly favors well-aligned ICDs, with a Positional Context Factor designed to counteract ICD biases. This more selective, balanced use of ICDs boosts accuracy and stability in multimodal ICL. Through evaluations across four LVLMs and six benchmarks, CAMA consistently achieves superior performance, validating both its effectiveness and generality.

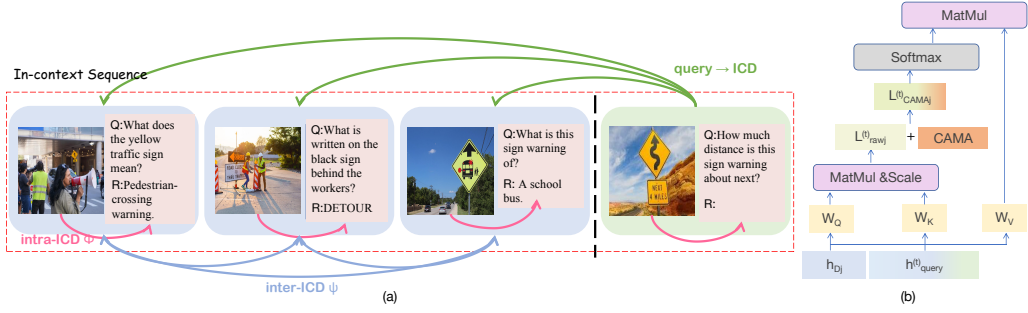


Figure 1: (a) An example of 3-shot in-context sequence and three standard attention limitations. (b) Overview of our attention-calibration method, CAMA. CAMA is a training-free method for directly modifying attention logits.

## 2 Limitations of Standard Attention

We study ICL in an interleaved image-text setting. Each ICD comprises an image, a textual query, and its ground-truth response, denoted by  $I$ ,  $Q$  and  $R$ , respectively. During ICL, a pretrained LVLM  $\mathcal{M}$  generates  $\hat{R}$  given an in-context sequence. Each sequence consists of an optional textual instruction  $Inst$ , a set of  $N$  ICDs and a query sample  $(\hat{I}, \hat{Q})$ . The  $i$ -th ICD is denoted as  $D_i = (I_i, Q_i, R_i)$ . Formally, ICL is represented as:

$$\hat{R} \leftarrow \mathcal{M}\{Inst; D_1, D_2 \dots, D_N; (\hat{I}, \hat{Q})\}. \quad (1)$$

As  $\mathcal{M}$  employs an LLM to jointly process visual and textual tokens, its generation of  $\hat{R}$  can be formulated in an autoregressive manner, with the attention mechanism at its core. At each generation step  $t$ , to predict the next token  $\hat{R}_t$ , the decoder computes a query state  $h_{query}^{(t)}$ , which is the hidden representation of the last token  $\hat{R}_{t-1}$ , encoding the query context and the partial response  $\hat{R}_{<t}$ . The raw attention logit  $L_{raw_j}^{(t)}$  quantifying the relevance of the  $j$ -th ICD  $D_j$  to  $h_{query}^{(t)}$  is computed as:

$$L_{raw_j}^{(t)} = \frac{(h_{query}^{(t)} W_Q)(h_{D_j} W_K)^T}{\sqrt{d_k}}, \quad (2)$$

where  $W_Q, W_K \in \mathbb{R}^{d_{model} \times d_k}$  are learnable linear projections.  $h_{D_j}$  is the hidden state of the last response token in  $D_j$ , obtained after processing its interleaved visual and textual tokens. These logits, after Softmax normalization, dictate the influence of each  $D_j$  on predicting  $\hat{R}_t$ , thereby enabling  $\mathcal{M}$  to infer task-specific patterns from the sequence.

Despite its central role, standard attention in multi-modal ICL faces inherent limitations that can impede optimal performance. A primary issue is the quality and utility of each  $h_{D_j}$ . The representational integrity of  $h_{D_j}$  depends critically on the **intra-ICD** cross-modal alignment, i.e., the robust

grounding of its textual components within its visual context. We denote this alignment quality by:

$$\Phi(D_j) = f(\mathcal{A}_{intra}((Q_j, R_j) \leftrightarrow I_j)) \quad (3)$$

where  $\mathcal{A}_{intra}$  measures the strength of internal text-image attention, and  $f$  is a function mapping these patterns to a scalar quality score. If  $\mathcal{A}_{intra}$  is weak,  $\Phi(D_j)$  will be low and  $D_j$  becomes a less faithful ICD. Yet the raw logit  $L_{raw_j}^{(t)}$  (as defined in Eq.(2)) does not explicitly factor in  $\Phi(D_j)$ .

Meanwhile, in ICL, modulating the model’s attention to different ICDs based on the query sample is critical. However, LVLM attention often fails to realize precise **query**→**ICD** interaction. The raw logit  $L_{raw_j}^{(t)}$  might not solely reflect the true multi-modal relevance  $Rel(S_Q, D_j)$  essential for the specific reasoning demands of the query sample  $S_Q$ . Instead,  $L_{raw_j}^{(t)}$  is often confounded by superficial unimodal cues (Tang et al., 2023) or systemic positional biases (Tian et al., 2025). Therefore, ICDs that contain misleading features or occupy specific positions within the sequence may unduly influence the attention distribution, leading the model to overweight less informative ICDs.

Furthermore, standard attention mechanisms, by computing  $L_{raw_j}$  predominantly based on pairwise query-ICD interactions prior to global normalization, lack explicit modeling of higher-order **inter-ICD** influences, such as synergy or redundancy. The collective utility of the ICD set  $\mathcal{D}$  for answering  $S_Q$  is often non-additive (Li, 2025). Let  $\Psi(D_j | \mathcal{D}_{-j}, S_Q)$  represent the synergistic value of  $D_j$  given other ICDs  $\mathcal{D}_{-j}$  and the query sample  $S_Q$ . The Softmax normalization does not inherently optimize for an ICD weighting that maximizes  $\sum_j W_j \Psi(D_j | \mathcal{D}_{-j}, S_Q)$ .

## 3 Method

The above three limitations in LVLM attention require refined calibration strategies that go beyond

prompt engineering. To this end, we introduce Context-Aware Modulated Attention (CAMA), which directly adjusts the raw attention logits. CAMA is a training-free, inference-time approach that recalibrates the raw attention logits  $L_{raw_j}^{(t)}$  before the Softmax normalization. This modulation aims to foster a more discerning and robust utilization of in-context sequence. CAMA integrates two principal components: a Query-ICD Joint Affinity Score and a Positional Context Factor.

### 3.1 Query-ICD Joint Affinity Score ( $J_j$ )

We first position more precise query  $\rightarrow$  ICD interaction as the core of CAMA by introducing the Query-ICD Joint Affinity Score ( $J_j$ ) as a metric to accurately assess the holistic relevance of each ICD to the query sample. To further foster robust intra-ICD alignment, its computation emphasizes joint multimodal alignment between image-text pairs rather than relying on unimodal features. A high  $J_j$  both signals reliable matching to the query and implicitly rewards ICDs with high internal coherence  $\Phi(D_j)$ , ensuring clear reasoning exemplars.

We derive fused multimodal embeddings  $E^Q$  for the query and  $E_j^D$  for each demonstration’s image-question pair. This is achieved by first encoding their respective visual and textual components using pre-trained CLIP encoders, denoted as  $\mathcal{E}^{vis}(\cdot)$  for images and  $\mathcal{E}^{txt}(\cdot)$  for text, followed by a fusion operation. Specifically, the fused query embeddings are computed as:

$$E^Q = \text{Norm}((\mathcal{E}^{vis}(\hat{I})) + (\mathcal{E}^{txt}(\hat{Q}))), \quad (4)$$

$$E_j^D = \text{Norm}((\mathcal{E}^{vis}(I_j)) + (\mathcal{E}^{txt}(Q_j))), \quad (5)$$

where  $\text{Norm}(\cdot)$  denotes L2 normalization. The joint affinity score  $J_j$  is then computed as the cosine similarity between these fused embeddings:

$$J_j = \text{cosine\_similarity}(E^Q, E_j^D). \quad (6)$$

The scores  $J_j$  are then normalized across all  $N$  ICDs using min-max scaling to the range  $[0, 1]$ , yielding  $J'_j$ .  $J'_j$  serves as a direct measure of the query-specific grounded utility of ICD  $D_j$ .

### 3.2 Positional Context Factor ( $P_j$ )

To counteract systemic positional biases and to enhance the LVLM’s overall perception of ICDs within the sequence, CAMA incorporates a Positional Context Factor  $P_j$ . Motivated by (Baldassini et al., 2024), which points out that ICDs closer to

the query sample more easily interfere with inter-ICD influences, we attempt to enable the model to attend more evenly to all ICDs. Thus,  $P_j$  adjusts an ICD’s salience based on its ordinal position  $pos_j \in \{1, \dots, N\}$  within the sequence:

$$P_j = \left( \frac{N - pos_j + 1}{N} \right)^k, \quad (7)$$

where  $N$  is the total number of ICDs. The exponent  $k \geq 0$  is a hyperparameter that dictates the shape of the positional compensation curve, which is optimized based on attention entropy.

### 3.3 Answer Generation with CAMA

After computing  $J'_j$  and  $P_j$ , we calibrate the raw attention logits  $L_{raw_j}^{(t)}$  at generation step  $t$  via an additive adjustment in the logit space, controlled by a single hyperparameter  $\lambda$ :

$$L_{CAMA_j}^{(t)} = L_{raw_j}^{(t)} + \lambda_J \cdot \log(J'_j + \epsilon) + \lambda_P \cdot \log(P_j + \epsilon), \quad (8)$$

where  $\epsilon$  is a small constant for numerical stability. The hyperparameters  $\lambda_J \geq 0$  and  $\lambda_P \geq 0$  independently control the calibration strength. Setting both to 0 recovers the original attention.

By modulating logits in this manner, CAMA encourages the LVLM to focus on ICDs that are both highly relevant to the query sample and less susceptible to suppression by positional bias. While CAMA does not explicitly model the inter-ICD synergy factor  $\Psi(D_j | \mathcal{D}_{-j}, S_Q)$  with a separate score, by ensuring a more accurate and equitable attention distribution across all relevant ICDs, it provides the base LVLM with a richer, less biased contextual input. This, in turn, enhances the LVLM’s intrinsic capacity to synthesize complementary information from the attended ICDs during its reasoning.

The final CAMA-calibrated attention logits  $L_{CAMA}^{(t)} = \{L_{CAMA_1}^{(t)}, \dots, L_{CAMA_N}^{(t)}\}$  are normalized using the Softmax function to produce the CAMA attention weights  $\alpha_{CAMA_j}^{(t)}$ :

$$\alpha_{CAMA_j}^{(t)} = \frac{\exp(L_{CAMA_j}^{(t)})}{\sum_{m=1}^N \exp(L_{CAMA_m}^{(t)})}. \quad (9)$$

These weights are then used by the LVLM’s decoder to form an aggregated context vector which guides the generation of the subsequent token  $\hat{R}_t$  of the answer. CAMA’s plug-and-play nature allows efficient integration into open-source LVLMs by modulating their attention at inference time.

LVLMM	method	VQAv2	VizWiz	OK-VQA	GQA	TextVQA	CLEVR	Avg.
LLaVA-NeXT	Standard	61.86	37.64	57.63	55.38	61.93	16.50	48.49
	+SoFA	63.21	38.09	58.14	57.42	62.28	14.29	48.90
	+CAMA	<b>64.03</b>	<b>39.21</b>	<b>59.51</b>	<b>58.39</b>	<b>62.89</b>	<b>17.28</b>	<b>50.22</b>
Idefics2	Standard	57.32	38.46	43.60	57.49	70.02	34.61	50.25
	+SoFA	59.04	38.95	46.12	57.75	72.31	35.54	51.62
	+CAMA	<b>60.17</b>	<b>39.27</b>	<b>46.64</b>	<b>59.26</b>	<b>73.47</b>	<b>36.29</b>	<b>52.52</b>
InternVL2.5	Standard	69.58	58.27	62.32	67.21	80.29	56.91	65.76
	+SoFA	70.85	59.62	62.48	68.30	82.75	59.12	67.19
	+CAMA	<b>72.09</b>	<b>61.72</b>	<b>65.47</b>	<b>70.03</b>	<b>84.26</b>	<b>61.07</b>	<b>69.11</b>
Qwen2.5VL	Standard	71.94	57.39	65.70	82.31	83.61	62.83	70.63
	+SoFA	72.31	59.06	67.28	84.52	84.34	64.85	72.06
	+CAMA	<b>74.25</b>	<b>60.26</b>	<b>68.37</b>	<b>84.97</b>	<b>86.73</b>	<b>65.79</b>	<b>73.40</b>

Table 1: Accuracy of 8-shot multimodal ICL on six benchmarks for four LVLMMs under three attention configurations: standard attention, SoFA-enhanced attention, and CAMA-enhanced attention. The highest values are in **bold**.

## 4 Experiments

### 4.1 Settings

Following multimodal ICL evaluation protocols (Awadalla et al., 2023; Laurençon et al., 2024a), we conduct experiments on three VQA benchmarks—VQAv2 (Goyal et al., 2017), VizWiz (Gurari et al., 2018), and OK-VQA (Marino et al., 2019). To further assess our method’s generalization, we also evaluate on GQA (Hudson and Manning, 2019), TextVQA (Singh et al., 2019), and the CLEVR subset of the VL-ICL bench (Zong et al., 2025). All validation-set instances serve as query samples. For each query, we uniformly sample eight examples from the corresponding training set as ICD, thereby forming an 8-shot sequence. We measure ICL performance across four advanced LVLMMs: LLaVA-NeXT-Interleave-7B (Li et al., 2024), Idefics2-8B (Laurençon et al., 2024b), InternVL2.5-8B (Chen et al., 2025), and Qwen2.5VL-7B (Bai et al., 2025).

We adopt SoFA (Tian et al., 2025) as our baseline, which is introduced in Appendix C. We set  $\epsilon = 1e-6$ . For each task, we tune the optimal hyperparameter values for both SoFA and CAMA on a small validation set of 100 samples, and the configurations used in our main experiments are detailed in Appendix D. Both methods are applied to every two layers of the LVLMM, while preserving standard causal attention in the remaining layers.

### 4.2 Main Results

Table 1 presents accuracy results for four LVLMMs across six benchmarks under three attention configurations. CAMA consistently achieves the highest accuracy, averaging a 2.53% gain over standard attention. Notably, stronger models benefit even more: InternVL2.5 and Qwen2.5VL see improvements of 3.35% and 2.77%, respectively, compared

to 1.73% on LLaVA-NeXT and 2.27% on Idefics2. These findings demonstrate CAMA’s ability to enhance both emerging and high-performance commercial LVLMMs, highlighting its practical applicability. Moreover, by outperforming SoFA’s causal-mask-based method, CAMA confirms the effectiveness of calibrating intermediate attention logits.

### 4.3 Ablation Study

	VQAv2	VizWiz	OK-VQA	GQA	TextVQA	CLEVR
$\lambda_J = 0.70$						
$\lambda_P = 0$	66.58	49.06	58.71	67.29	76.12	43.72
$\lambda_P = 0.25$	67.48	49.98	59.51	66.87	<b>76.93</b>	44.53
$\lambda_P = 0.50$	67.19	50.13	59.15	66.74	76.28	45.09
$\lambda_P = 0.40$						
$\lambda_J = 0$	65.41	48.25	57.28	65.73	74.28	43.89
$\lambda_J = 0.5$	<b>67.72</b>	50.31	<b>59.72</b>	67.68	76.57	<b>45.32</b>
$\lambda_J = 1.0$	67.18	<b>50.34</b>	59.09	<b>68.26</b>	76.37	44.62

Table 2: The results of 8-shot ICL with CAMA varying the value of  $\lambda_J$  and  $\lambda_P$ . The highest values are in **bold**.

Table 2 shows results when fixing one of  $\lambda_J$  and  $\lambda_P$  and varying the other. Ablating  $J_j$  causes a larger performance drop than ablating  $P_j$  indicating the critical importance of modal alignment and query-sample-guided attention. While the optimal parameter combination varies across datasets, the overall performance fluctuation is minor, underscoring CAMA’s robustness. Additionally, Appendix F explores the impact of varying  $k$ , ICD shot count, and retrieval strategy on CAMA.

## 5 Conclusion

In this paper, we propose CAMA, a plug-and-play, training-free attention calibration method that combines a query-ICD joint affinity score with a positional context factor. CAMA refines inference-time attention to mitigate three key limitations of standard attention that impede effective multimodal ICL. Experiments on four LVLMMs in six benchmarks prove that CAMA effectively yields consistent performance gains over baseline methods.

## Limitations

Although we examine inter-ICD influences as a limitation of standard attention in Section 2 and define the synergistic value  $\Psi(D_j|\mathcal{D}_{-j}, S_Q)$  to quantify each ICD’s contribution, CAMA does not explicitly resolve this issue; instead, it indirectly mitigates it via positional compensation  $P_j$ . Modeling the complex inter-ICD dynamics, which may include reinforcement, complementarity and even exclusion, under a purely training-free regime is challenging. In future work, we will explore lightweight training schemes or targeted causal-mask modifications to more finely address this limitation.

## References

- Jean-Baptiste Alayrac, Jeff Donahue, Pauline Luc, Antoine Miech, Iain Barr, Yana Hasson, Karel Lenc, Arthur Mensch, Katherine Millican, Malcolm Reynolds, et al. 2022. Flamingo: a visual language model for few-shot learning. *Advances in neural information processing systems*, 35:23716–23736.
- Anas Awadalla, Irena Gao, Josh Gardner, Jack Hessel, Yusuf Hanafy, Wanrong Zhu, Kalyani Marathe, Yonatan Bitton, Samir Gadre, Shiori Sagawa, Jenia Jitsev, Simon Kornblith, Pang Wei Koh, Gabriel Ilharco, Mitchell Wortsman, and Ludwig Schmidt. 2023. [Openflamingo: An open-source framework for training large autoregressive vision-language models](#).
- Jinze Bai, Shuai Bai, Shusheng Yang, Shijie Wang, Sinan Tan, Peng Wang, Junyang Lin, Chang Zhou, and Jingren Zhou. 2023. Qwen-vl: A frontier large vision-language model with versatile abilities. *arXiv preprint arXiv:2308.12966*, 1(2):3.
- Shuai Bai, Keqin Chen, Xuejing Liu, Jialin Wang, Wenbin Ge, Sibao Song, Kai Dang, Peng Wang, Shijie Wang, Jun Tang, Humen Zhong, Yuanzhi Zhu, Mingkun Yang, Zhaohai Li, Jianqiang Wan, Pengfei Wang, Wei Ding, Zheren Fu, Yiheng Xu, Jiabo Ye, Xi Zhang, Tianbao Xie, Zesen Cheng, Hang Zhang, Zhibo Yang, Haiyang Xu, and Junyang Lin. 2025. [Qwen2.5-vl technical report](#).
- Folco Bertini Baldassini, Mustafa Shukor, Matthieu Cord, Laure Soulier, and Benjamin Piwowarski. 2024. What makes multimodal in-context learning work? In *Proceedings of the IEEE/CVF Conference on Computer Vision and Pattern Recognition*, pages 1539–1550.
- Rahul Atul Bhope, Praveen Venkateswaran, K. R. Jayaram, Vatche Isahagian, Vinod Muthusamy, and Nalini Venkatasubramanian. 2025. [Optiseq: Ordering examples on-the-fly for in-context learning](#).
- Tom B. Brown, Benjamin Mann, Nick Ryder, Melanie Subbiah, Jared Kaplan, Prafulla Dhariwal, Arvind Neelakantan, Pranav Shyam, Girish Sastry, Amanda Askell, Sandhini Agarwal, Ariel Herbert-Voss, Gretchen Krueger, Tom Henighan, Rewon Child, Aditya Ramesh, Daniel M. Ziegler, Jeffrey Wu, Clemens Winter, Christopher Hesse, Mark Chen, Eric Sigler, Mateusz Litwin, Scott Gray, Benjamin Chess, Jack Clark, Christopher Berner, Sam McCandlish, Alec Radford, Ilya Sutskever, and Dario Amodei. 2020. [Language models are few-shot learners](#).
- Zhe Chen, Weiyun Wang, Yue Cao, Yangzhou Liu, Zhangwei Gao, Erfei Cui, Jinguo Zhu, Shenglong Ye, Hao Tian, Zhaoyang Liu, Lixin Gu, Xuehui Wang, Qingyun Li, Yimin Ren, Zixuan Chen, Jiapeng Luo, Jiahao Wang, Tan Jiang, Bo Wang, Conghui He, Botian Shi, Xingcheng Zhang, Han Lv, Yi Wang, Wenqi Shao, Pei Chu, Zhongying Tu, Tong He, Zhiyong Wu, Huipeng Deng, Jiaye Ge, Kai Chen, Kaipeng Zhang, Limin Wang, Min Dou, Lewei Lu, Xizhou Zhu, Tong Lu, Dahua Lin, Yu Qiao, Jifeng Dai, and Wenhai Wang. 2025. [Expanding performance boundaries of open-source multimodal models with model, data, and test-time scaling](#).
- Damai Dai, Yutao Sun, Li Dong, Yaru Hao, Shuming Ma, Zhifang Sui, and Furu Wei. 2022. Why can gpt learn in-context? language models implicitly perform gradient descent as meta-optimizers. *arXiv preprint arXiv:2212.10559*.
- Qingxiu Dong, Lei Li, Damai Dai, Ce Zheng, Jingyuan Ma, Rui Li, Heming Xia, Jingjing Xu, Zhiyong Wu, Tianyu Liu, Baobao Chang, Xu Sun, Lei Li, and Zhifang Sui. 2024. [A survey on in-context learning](#).
- Sivan Doherty, Shaked Perek, M Jehanzeb Mirza, Wei Lin, Amit Alfassy, Assaf Arbelle, Shimon Ullman, and Leonid Karlinsky. 2024a. Towards multimodal in-context learning for vision & language models. *arXiv preprint arXiv:2403.12736*.
- Sivan Doherty, Shaked Perek, M Jehanzeb Mirza, Wei Lin, Amit Alfassy, Assaf Arbelle, Shimon Ullman, and Leonid Karlinsky. 2024b. Towards multimodal in-context learning for vision & language models. *arXiv preprint arXiv:2403.12736*.
- Tianyu Gao, Adam Fisch, and Danqi Chen. 2021. [Making pre-trained language models better few-shot learners](#).
- Yash Goyal, Tejas Khot, Douglas Summers-Stay, Dhruv Batra, and Devi Parikh. 2017. Making the V in VQA matter: Elevating the role of image understanding in Visual Question Answering. In *Conference on Computer Vision and Pattern Recognition (CVPR)*.
- Qi Guo, Leiyu Wang, Yidong Wang, Wei Ye, and Shikun Zhang. 2024. What makes a good order of examples in in-context learning. In *Findings of the Association for Computational Linguistics: ACL 2024*, pages 14892–14904.
- Danna Gurari, Qing Li, Abigale J. Stangl, Anhong Guo, Chi Lin, Kristen Grauman, Jiebo Luo, and Jeffrey P.

- Bigham. 2018. [Vizwiz grand challenge: Answering visual questions from blind people](#).
- Roe Hendel, Mor Geva, and Amir Globerson. 2023. In-context learning creates task vectors. *arXiv preprint arXiv:2310.15916*.
- Drew A. Hudson and Christopher D. Manning. 2019. [Gqa: A new dataset for real-world visual reasoning and compositional question answering](#).
- Hugo Laurençon, Andrés Marafioti, Victor Sanh, and Léo Tronchon. 2024a. [Building and better understanding vision-language models: insights and future directions](#).
- Hugo Laurençon, Léo Tronchon, Matthieu Cord, and Victor Sanh. 2024b. [What matters when building vision-language models?](#)
- Feng Li, Renrui Zhang, Hao Zhang, Yuanhan Zhang, Bo Li, Wei Li, Zejun Ma, and Chunyuan Li. 2024. [Llava-next-interleave: Tackling multi-image, video, and 3d in large multimodal models](#).
- Li Li, Jiawei Peng, Huiyi Chen, Chongyang Gao, and Xu Yang. 2023a. [How to configure good in-context sequence for visual question answering](#).
- Xiaonan Li, Kai Lv, Hang Yan, Tianyang Lin, Wei Zhu, Yuan Ni, Guotong Xie, Xiaoling Wang, and Xipeng Qiu. 2023b. [Unified demonstration retriever for in-context learning](#).
- Yanshu Li. 2025. [Advancing multimodal in-context learning in large vision-language models with task-aware demonstrations](#). *arXiv preprint arXiv:2503.04839*.
- Yanshu Li, Hongyang He, Yi Cao, Qisen Cheng, Xiang Fu, and Ruixiang Tang. 2025. [M2iv: Towards efficient and fine-grained multimodal in-context learning in large vision-language models](#). *arXiv preprint arXiv:2504.04633*.
- Haotian Liu, Chunyuan Li, Qingyang Wu, and Yong Jae Lee. 2023a. [Visual instruction tuning](#). *Advances in neural information processing systems*, 36:34892–34916.
- Jiachang Liu, Dinghan Shen, Yizhe Zhang, Bill Dolan, Lawrence Carin, and Weizhu Chen. 2021. [What makes good in-context examples for gpt-3?](#)
- Sheng Liu, Haotian Ye, Lei Xing, and James Zou. 2023b. [In-context vectors: Making in context learning more effective and controllable through latent space steering](#). *arXiv preprint arXiv:2311.06668*.
- Shi Liu, Kecheng Zheng, and Wei Chen. 2024. [Paying more attention to image: A training-free method for alleviating hallucination in lvlms](#).
- Yao Lu, Max Bartolo, Alastair Moore, Sebastian Riedel, and Pontus Stenetorp. 2022. [Fantastically ordered prompts and where to find them: Overcoming few-shot prompt order sensitivity](#).
- Kenneth Marino, Mohammad Rastegari, Ali Farhadi, and Roozbeh Mottaghi. 2019. [Ok-vqa: A visual question answering benchmark requiring external knowledge](#).
- Sewon Min, Xinxu Lyu, Ari Holtzman, Mikel Artetxe, Mike Lewis, Hannaneh Hajishirzi, and Luke Zettlemoyer. 2022. [Rethinking the role of demonstrations: What makes in-context learning work?](#) *arXiv preprint arXiv:2202.12837*.
- Jane Pan. 2023. [What in-context learning “learns” in-context: Disentangling task recognition and task learning](#). Master’s thesis, Princeton University.
- Yingzhe Peng, Xinting Hu, Jiawei Peng, Xin Geng, Xu Yang, et al. 2024. [Live: Learnable in-context vector for visual question answering](#). *Advances in Neural Information Processing Systems*, 37:9773–9800.
- Kiran Purohit, Venkatesh V, Raghuram Devalla, Krishna Mohan Yerragorla, Sourangshu Bhattacharya, and Avishek Anand. 2024. [Explora: Efficient exemplar subset selection for complex reasoning](#).
- Amanpreet Singh, Vivek Natarajan, Meet Shah, Yu Jiang, Xinlei Chen, Dhruv Batra, Devi Parikh, and Marcus Rohrbach. 2019. [Towards vqa models that can read](#).
- Ruixiang Tang, Dehan Kong, Longtao Huang, and Hui Xue. 2023. [Large language models can be lazy learners: Analyze shortcuts in in-context learning](#). *arXiv preprint arXiv:2305.17256*.
- Xinyu Tian, Shu Zou, Zhaoyuan Yang, and Jing Zhang. 2025. [Identifying and mitigating position bias of multi-image vision-language models](#). *arXiv preprint arXiv:2503.13792*.
- Eric Todd, Millicent L Li, Arnab Sen Sharma, Aaron Mueller, Byron C Wallace, and David Bau. 2023. [Function vectors in large language models](#). *arXiv preprint arXiv:2310.15213*.
- Jason Wei, Xuezhi Wang, Dale Schuurmans, Maarten Bosma, Brian Ichter, Fei Xia, Ed Chi, Quoc Le, and Denny Zhou. 2023. [Chain-of-thought prompting elicits reasoning in large language models](#).
- Zhiyong Wu, Yaoxiang Wang, Jiacheng Ye, and Lingpeng Kong. 2022. [Self-adaptive in-context learning: An information compression perspective for in-context example selection and ordering](#). *arXiv preprint arXiv:2212.10375*.
- Sang Michael Xie, Aditi Raghunathan, Percy Liang, and Tengyu Ma. 2021. [An explanation of in-context learning as implicit bayesian inference](#). *arXiv preprint arXiv:2111.02080*.
- Zhichao Xu, Daniel Cohen, Bei Wang, and Vivek Srikumar. 2024. [In-context example ordering guided by label distributions](#). *arXiv preprint arXiv:2402.11447*.

Xu Yang, Yongliang Wu, Mingzhuo Yang, Haokun Chen, and Xin Geng. 2024. [Exploring diverse in-context configurations for image captioning](#).

Qinghao Ye, Haiyang Xu, Guohai Xu, Jiabo Ye, Ming Yan, Yiyang Zhou, Junyang Wang, Anwen Hu, Pengcheng Shi, Yaya Shi, et al. 2023. [mplug-owl: Modularization empowers large language models with multimodality](#). *arXiv preprint arXiv:2304.14178*.

Anhao Zhao, Fanghua Ye, Jinlan Fu, and Xiaoyu Shen. 2024. [Unveiling in-context learning: A coordinate system to understand its working mechanism](#). *arXiv preprint arXiv:2407.17011*.

Denny Zhou, Nathanael Schärli, Le Hou, Jason Wei, Nathan Scales, Xuezhi Wang, Dale Schuurmans, Claire Cui, Olivier Bousquet, Quoc Le, and Ed Chi. 2023. [Least-to-most prompting enables complex reasoning in large language models](#).

Yongshuo Zong, Ondrej Bohdal, and Timothy Hospedales. 2025. [Vl-icl bench: The devil in the details of multimodal in-context learning](#).

## A Related Works

**In-context Learning (ICL).** ICL refers to a model’s ability to tackle new tasks by conditioning on a sequence of input–output examples without any parameter updates (Brown et al., 2020; Dong et al., 2024). Its training-free nature and minimal annotation requirements have driven widespread adoption in NLP, greatly accelerating the deployment of Large Language Models (LLMs) (Wei et al., 2023). Inspired by this success, recent work has extended ICL to the multimodal setting. To foster robust multimodal ICL, models like Flamingo employ specialized training and fine-tuning strategies (Alayrac et al., 2022; Awadalla et al., 2023). Commercial LVLMs, such as the QwenVL (Bai et al., 2025) and InternVL (Chen et al., 2025) series, now treat multimodal ICL as an essential ability. Yet, the intricate cross-modal interactions of multimodal ICL tasks remain a formidable challenge even for these state-of-the-art architectures.

**Enhancing Multimodal ICL.** Empirical studies show that the instability of the multimodal ICL arises from extreme sensitivity to the in-context sequence (Liu et al., 2021; Gao et al., 2021; Li et al., 2023b). In-context demonstration (ICD) selection, ordering and format can all greatly affect performance. This has driven two main optimization strategies: (1) retrieval-based selection, which scores each candidate example’s expected contribution to correct reasoning for a given query and picks the top- $n$  ICDs (Guo et al., 2024; Purohit et al., 2024; Li, 2025); and (2) sequence-reranking, which, given a fixed set of ICDs, applies a learned or hand-crafted metric to order them into the most effective in-context sequence (Wu et al., 2022; Xu et al., 2024; Bhoje et al., 2025). However, confined to prompt engineering and limited by the intrinsic capacities of LVLMs, these approaches produce only marginal gains on tasks that require complex reasoning. This underscores the need to more deeply leverage LVLMs’ internal reasoning mechanisms.

**ICL Mechanisms.** Xie et al. (2021) propose a theoretical framework that casts ICL as an implicit Bayesian inference process, while Dai et al. (2022) interpret it as performing gradient descent within an internal implicit model. Simultaneously, the role of ICDs in ICL has sparked debate: Min et al. (2022) contend that performance relies on explicit ICD features (e.g., label space), whereas Zhou et al. (2023) attribute success to the implicit input–output map-

pings embodied by the ICDs. Pan (2023) and Zhao et al. (2024) further attempt to integrate the cognitive and perceptual contributions of ICDs into a unified framework. These lines of inquiry highlight the intrinsic complexity of ICL, which is even more pronounced in multimodal settings. At a more granular level, task-vector methods have emerged to convert in-context sequences into vectors that directly modulate the model’s residual stream (Hendel et al., 2023; Todd et al., 2023; Liu et al., 2023b). However, adapting these techniques to multimodal domains generally requires additional training, reducing their efficiency (Peng et al., 2024; Li et al., 2025).

## B Caching Optimization

Since modulating attention incurs additional inference overhead, we introduce efficiency optimizations to CAMA to mitigate this issue. We implement a global caching mechanism by first projecting all demonstration hidden states through the shared key and value matrices and storing the resulting matrices  $\mathbf{K}_{\text{cache}} \in \mathbb{R}^{N \times d_k}$  and  $\mathbf{V}_{\text{cache}} \in \mathbb{R}^{N \times d_v}$  in low-precision on the GPU. During the same initialization, we compute and log-transform demonstration-level affinity and positional scalars, yielding  $\log J_{\text{cache}}$  and  $\log P_{\text{cache}}$ , which are likewise pinned in GPU memory. At each decoding step  $t$ , after computing the query vector  $q_t$ , we obtain the fused attention output in a single batched operation:

$$h_{\text{attn}} = \text{softmax} \left( \frac{q_t \mathbf{K}_{\text{cache}}^\top}{\sqrt{d_k}} + \lambda_J \log J_{\text{cache}} + \lambda_P \log P_{\text{cache}} \right) \mathbf{V}_{\text{cache}}. \quad (10)$$

By reusing these cached projections and bias terms across all Transformer layers and time steps, our approach eliminates redundant linear projections, similarity evaluations, and positional adjustments, enabling efficient, vectorized, mixed-precision multimodal ICL inference without modifying the underlying model architecture. These optimizations also demonstrate CAMA’s scalability.

## C Baseline:SoFA

Soft Attention (SoFA) is also a training-free and plug-and-play module for LVLMs that alleviates position bias by reshaping inter-image attention.

Specifically, rather than employing purely causal (unidirectional) attention among image tokens, SoFA defines a soft attention mask

$$M_{\text{soft}} = (1 - \sigma) \mathbf{1}_{\text{causal}} + \sigma \mathbf{1}_{\text{bidirectional}}, \quad (11)$$

and computes the resulting attention output as

$$H_{\text{soft}} = \text{Softmax} \left( \frac{QK^\top}{\sqrt{d}} \right) \odot M_{\text{soft}} V, \quad (12)$$

where  $\sigma \in [0, 1]$  controls the interpolation degree between causal and bidirectional masks and is selected via a small validation set. The interpolation is applied every two layers to preserve the model’s original training dynamics. By smoothing positional cues and reinforcing early-image interactions while preserving text autoregression, SoFA achieves balanced reasoning over all image positions and significantly reduces prediction inconsistency. It has also been found to improve the performance of multimodal ICL.

## D Configuration Details

LVLM	para.	VQA2	VizWiz	OK-VQA	GQA	TextVQA	CLEVR
LLaVA-NeXT	$\lambda_J$	0.82	0.94	0.75	0.62	0.51	0.95
	$\lambda_P$				0.48		
	$k$				0.75		
Idefics2	$\lambda_J$	0.87	0.95	0.80	0.58	0.47	0.92
	$\lambda_P$				0.60		
	$k$				0.87		
InternVL2.5	$\lambda_J$	0.76	0.81	0.75	0.57	0.46	0.83
	$\lambda_P$				0.41		
	$k$				0.52		
Qwen2.5VL	$\lambda_J$	0.73	0.69	0.68	0.52	0.37	0.81
	$\lambda_P$				0.35		
	$k$				0.32		

Table 3: Configuration of hyperparameters  $\lambda_J, \lambda_P$ , and  $k$  for the main experimental results in Table 1.

Table 3 presents the hyperparameter configurations for our main experiments.  $\lambda_P$  and  $k$  closely align with a model’s inherent inference capabilities, especially its long-context performance. Thus, we can assign a single  $\lambda_P$  and  $k$  per model. By contrast, the affinity weight  $\lambda_J$  is more task-specific, but its variation across models is modest. Thus, while CAMA requires some manual tuning, its parameter ranges remain stable across both tasks and models, reducing tuning overhead and enhancing generalization.

## E Visualization

We visualize image and text attention under different in context learning settings (Figure 2). CAMA enhances the model’s focus on critical visual regions and relevant tokens such as “warning,” confirming its effectiveness. Ablation studies show

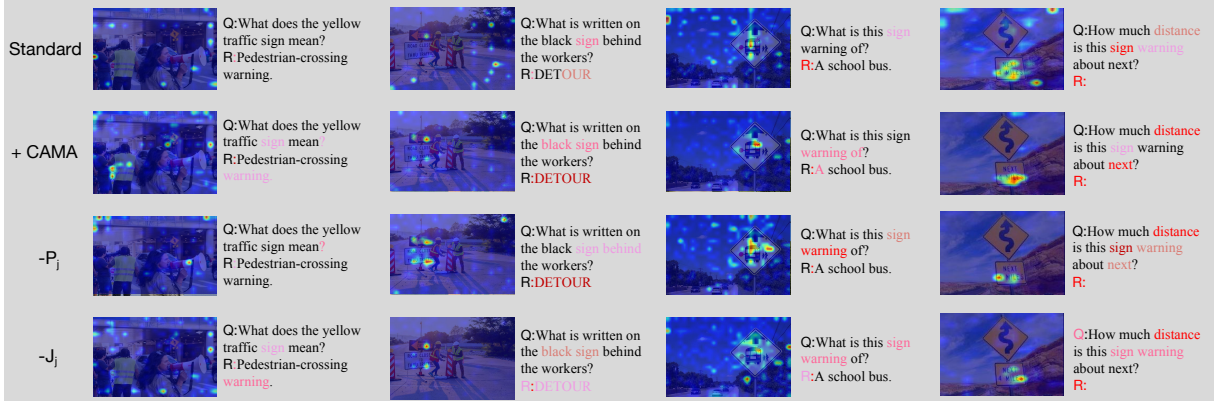


Figure 2: Visualization of Idefics2’s image and text attention maps under four attention settings: Standard, +CAMA, +CAMA w/o  $P_j$ , and +CAMA w/o  $J_j$ . Darker regions indicate stronger model attention.

that incorporating  $J_j$  improves alignment and localization of salient features, while incorporating  $P_j$  yields a more uniform attention distribution across ICDs and reduces positional bias. Nevertheless, attention still concentrates on ICDs nearest the query sample, indicating that further techniques such as masking are needed to fully address positional bias.

## F Additional Ablation Studies

### F.1 Diverse $k$

$k$	VQAv2	VizWiz	OK-VQA	GQA	TextVQA	CLEVR
0.25	67.20	48.97	59.54	67.71	77.03	44.47
0.50	<b>67.51</b>	<b>49.62</b>	<b>60.13</b>	67.48	76.92	<b>44.83</b>
0.75	67.47	47.82	59.72	68.27	<b>77.57</b>	44.69
1.00	66.95	48.26	57.84	<b>68.30</b>	77.28	42.85

Table 4: The results of 8-shot ICL with CAMA varying the value of  $k$ . The highest values are in **bold**.

The choice of  $k$  reflects a trade-off between mitigating inherent positional bias and fully leveraging all demonstration information. Our results show that moderate values of  $k$  (e.g., 0.50 or 0.75) strike an effective balance on most VQA datasets, boosting the relative importance of early demonstrations and thereby improving ICL performance. However, certain tasks, such as TextVQA can benefit from a stronger emphasis on early examples, owing to their unique characteristics or task-specific bias patterns. This behavior depends on each dataset’s task format and distribution; nonetheless, tuning  $k$  should be guided primarily by the model’s intrinsic capabilities.

### F.2 Diverse Shot of ICDs

In the main experiments, we employed 8-shot in-context sequences. Here, we study the effect of

Shot	VQAv2	VizWiz	OK-VQA	GQA	TextVQA	CLEVR
4	63.47	45.82	56.88	64.29	73.60	43.71
	+1.87	+2.05	+2.28	+1.45	+1.72	+2.15
8	67.64	50.12	60.00	68.16	76.84	45.11
	+2.46	+2.18	+2.69	+2.56	+2.88	+2.40
16	71.97	51.28	63.49	72.51	78.19	44.27
	+3.02	+2.71	+1.85	+2.80	+3.06	+2.54

Table 5: Average performance of CAMA on four LVLMs using 4-, 8-, and 16-shot in-context sequences. Values below each score indicate the improvement over standard attention.

ICD count on CAMA’s performance. As shown in Table 5, CAMA consistently outperforms standard attention in 4-, 8-, and 16-shot settings, with gains of 1.45%–3.06%. Notably, each dataset shows a general trend of increasing gains with longer sequences. As discussed in Section 2, longer contexts exacerbate positional bias and impede the model’s ability to identify informative ICDs via query-guided attention. By mitigating both issues, CAMA proves its value for long-context multimodal ICL.

### F.3 Diverse Retrieval Strategies

Strategy	VQAv2	VizWiz	OK-VQA	GQA	TextVQA	CLEVR
RS	67.64	50.12	60.00	68.16	76.84	45.11
	+2.46	+2.18	+2.69	+2.56	+2.88	+2.40
I2I	66.41	51.26	60.37	69.54	77.09	45.28
	+3.35	+3.01	+2.75	+2.92	+2.73	+2.26
IQ2IQ	69.22	53.71	63.37	71.84	79.12	44.87
	+1.28	+1.76	+2.04	+1.63	+1.15	+0.94

Table 6: Average performance of CAMA on four LVLMs using RS, I2I, and IQ2IQ as strategies to configure in-context sequences. Values below each score indicate the improvement over standard attention.

In our main experiments, we construct in-context sequences via uniform random sampling (RS) from

the training set. RS is a simple, low-overhead strategy commonly used in practice. In contrast, more advanced retrieval-augmented generation (RAG) systems typically employ metric-based retrieval, most often leveraging embedding similarity. Concretely, we encode each example  $(I_i, Q_i, R_i)$  and the query sample  $(\hat{I}, \hat{Q})$  with CLIP’s visual and textual encoders, then compare embeddings in two ways:

- I2I: Compute similarity between the query image and each example image, retrieving the top-8 examples by image–image score.
- IQ2IQ: Concatenate each example’s image and question embeddings and the query’s embeddings, then retrieve the top-8 examples by joint image–text similarity.

As shown in Table 6, CAMA delivers consistent gains of 0.94%–3.35% across all three retrieval strategies. Its largest improvements occur when using random sampling (RS), likely because image-only retrieval can induce shortcut learning (Li et al., 2023a), where the model merely copies answers from visually similar ICDs rather than reasoning over their full input–output mappings. By modulating query-guided attention, CAMA promotes a holistic understanding of each ICD and mitigates reliance on isolated features, thereby boosting ICL performance. In contrast, gains under IQ2IQ retrieval are smaller, since joint image–text retrieval already approximates the Query–ICD Joint Affinity Score. Even so, by alleviating positional bias, CAMA still yields improvements.